A Method to Create a Single Photon LiDAR based Hydro-flattened DEM

Sagar Deshpande[1] and Alper Yilmaz[2]

[1] *Surveying Engineering, Ferris State University*
[2] *Department of Civil, Environmental, and Geodetic Engineering, The Ohio State University*

Abstract

A ground surface created over water bodies, using LiDAR points, appears unnatural. Hence, breaklines are added to LiDAR point cloud to create a hydro-flattened DEM or TIN surface. These breaklines add an even surface to the water bodies. Contours produced using such surface are consistent with the contours on traditional topographic maps. With the development in laser technology, new LiDAR sensors such as Single photon (SP) and Geiger mode LiDAR are available. In this paper, a SP LiDAR point cloud is evaluated for its needs to perform hydro-flattening and a method to hydro-flatten this data is presented.

A previously developed method for LM LiDAR, which is based on the intersection of two surfaces: the water surface and the bare ground surface, is adapted to perform hydro-flattening of the SP LiDAR points. SP LiDAR data, acquired over Hartford, Connecticut, is used in this study. First, a continuous bare ground surface (CBGS) is created using unclassified SP LiDAR points. A raster surface of 3 m grid size is created using the elevation of the lowest point. All the points within 0.5 m of this surface are used to create a bare ground surface. The grids with no elevation are assigned as low elevation points. The bare ground surface and the low points are combined to create a CBGS. Second, a virtual water surface is created by extracting the water surface elevations at cross-sections placed at regular intervals along the river centerline. Using these elevations, a virtual water surface is created which resembles the natural water profile. In the last

step, these two surfaces are intersected to extract the bank shoreline. After simplification, this raw shoreline is converted into a 3D feature and is used to hydro-flatten the SP LiDAR data. The results obtained are compared with orthoimages of the area.

1 Introduction

The traditional topographic maps, produced by the USGS using the national elevation dataset (NED), depicts the topography using contours. Although modern computer technology provides superior alternatives, the contour map remains a popular and widely used product. An example of the USGS topographic map is shown in Figure 1. This figure shows 10-ft interval contours

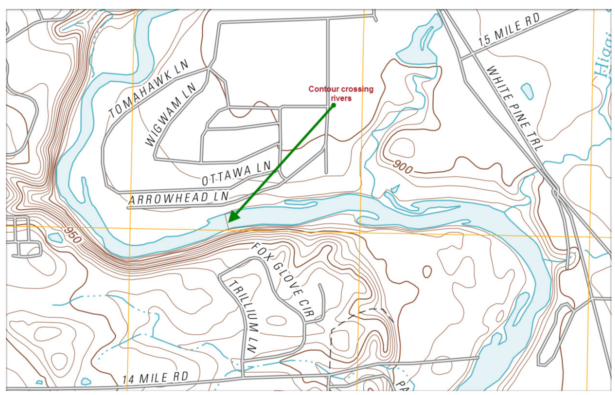

Figure 1: Clip of a USGS topographic map

which cross the river at every 10-ft rise in elevation along the river centerline.

On the other hand, the elevation along a river centerline from a LiDAR point cloud is irregular. A topographic map, created using a LiDAR-based TIN surface, would show contours crossing a water body at several locations. Such a topographic map would be inconsistent compared to the USGS national elevation dataset (NED). Therefore, there is a need to include a 3D hardline along the bank shoreline which resembles the actual water surface elevation at the time of data acquisition. Such a hardline would result in regular contours consistent with the traditional NED. Hence, hydro-flattening is the process of creating a LiDAR-based DEM in which water surfaces appear as they would in traditional topographic DEMs created from photogrammetric digital terrain models (DTMs) [4].

In this study, a method to hydro-flatten Single Photon LiDAR data is presented. The main objectives of this paper are to report the difference between traditional linear mode (LM) LiDAR and SP LiDAR with reference to the hydro-flattening properties and also to provide a methodology to hydro-flatten SP LiDAR data.

2 Background review

SP LiDAR sensors are an emerging technology which has been developed by Sigma Space corporation. The SP LiDAR works on the principle of splitting a single laser pulse into multiple sub-pulses to increase the density of the information reflected by a ground object. As explained in [1], segmented detectors, which are similar to the focal plane array design of a digital camera, are used to receive the back scattered sub-pulses, thereby increasing the point density to 15 to 30 points per square meter. This working principle is shown in Figure 2.

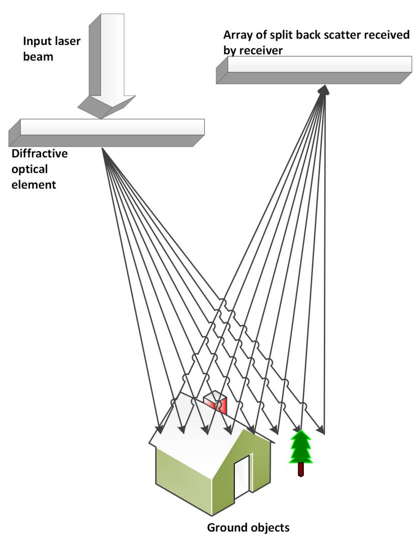

Figure 2: Working principle of a Single Photon LiDAR sensor

In a SP LiDAR system, single photon sensitivity is combined with timing receivers having nanosecond recovery times and a multistop timing capability per pixel [1]. These characteristics enable the SP LiDAR to operate under conditions of full solar illumination and to penetrate semi-porous obscurations such as vegetation, ground fog, thin clouds, etc. Also, the use of green (0.532 microns) laser proves to offer additional capability for water penetration (bathymetry) as the SP LiDAR system is able to routinely measure the surface of the water as well as the topography below the water. A cross-section view of the data is shown in Figure 3. This figure shows

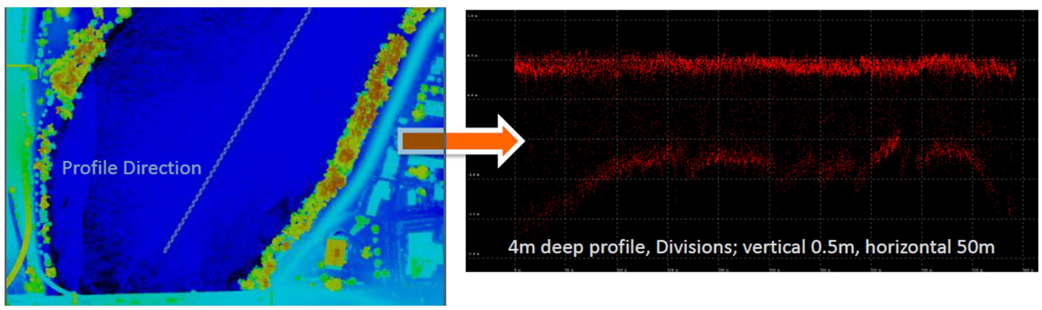

Figure 3: Water penetration capability of Single Photon LiDAR [7]

points along the profile direction. It can be seen in the longitudinal profile that the SP LiDAR points are not only available on but also beneath the water surface. As stated in [8], the exact bathymetric performance of the sensors is currently being calibrated and initial tests indicate a penetration of 15-20 meters. Compared to Linear mode LiDAR, it requires only a few photons to detect the returned signal, resulting in lower-power laser which can be flown from higher altitudes. Data over a wider swath can be acquired thereby reducing the data acquisition time.

Considering these factors, a study is conducted to determine how to hydro-flatten SP LiDAR data. Bare ground and all points TIN surfaces, created using SP LiDAR, are visually analyzed.

Figure 4(*b* and *c*), show the irregularities over the water surface, resulting in a displeasing cartographic appearance, similar to the LM LiDAR-based surface. Thus, it is concluded that hydro-flattening requirements developed for the LM LiDAR can be implemented on the SP LIDAR data.

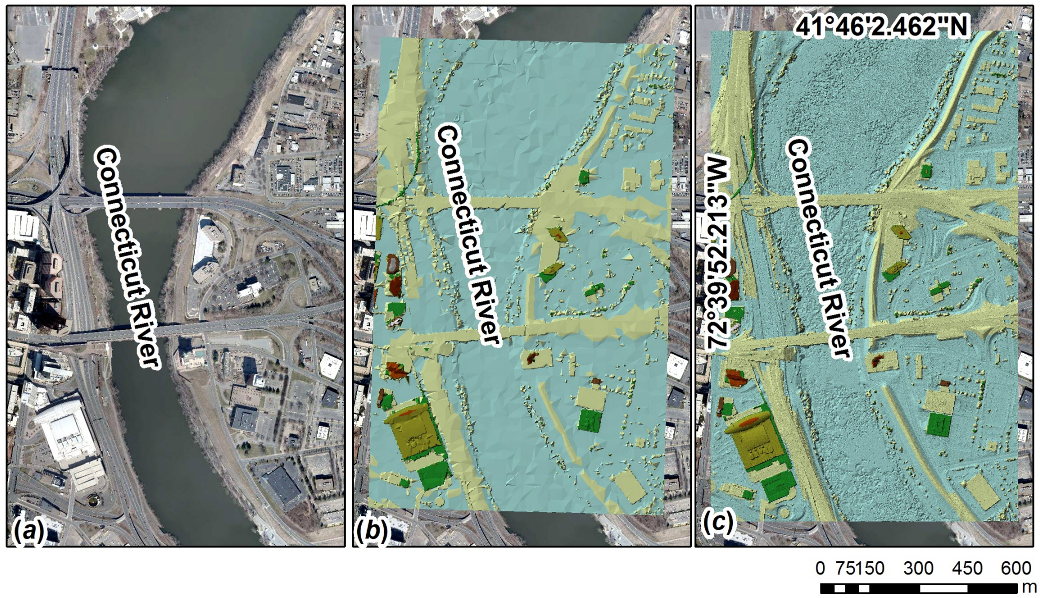

Figure 4: Overview of the Connecticut study area. (a) the orthoimage of the area, and the Connecticut river, (b) a TIN surface created using all the points, (c) a TIN surface created using the points within 0.5 m of the bare ground surface.

3 Data used

SP-LiDAR points collected over the Connecticut River, Hartford, Connecticut are used in this study. This data is not classified as ground or non-ground by the vendor. From Figure 4, it can be noted that this data is in an urban area and two bridges exist across within the extents. The point density of this data is more than 18 points/m^2, thereby exceeding the QL0 category [4].

Figure 4(a) shows the orthoimages used for the visual inspection of the results. These images and their metadata were downloaded from the Connecticut Environmental conditions online website. According to the metadata, the orthoimages were acquired in 2009 at a spatial resolution of 7.62 cm (3-inches) and meets the horizontal accuracy of ASPRS Class I.

4 Methodology

The methodology, proposed in [3], is adapted to use for the SP LiDAR point cloud. This methology is divided into four steps: Conditioned ground surface creation, water surface estimation, bank shoreline determination, and hydro-flattening.

4.1 Conditioned ground surface creation

In this methodology, out of the several methods available to create a bare ground surface [6], an approach proposed in [2] is adapted. Figure 5 shows the methodology.

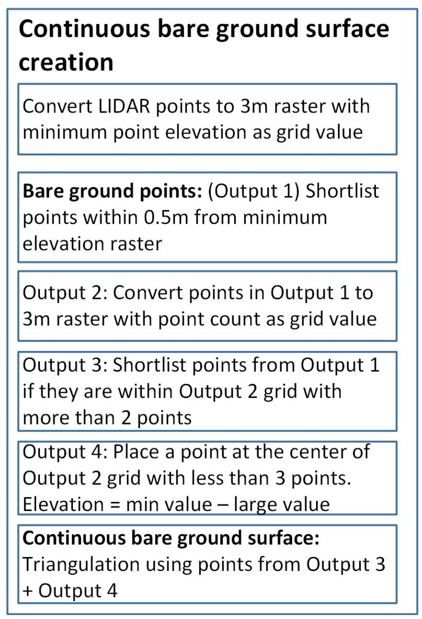

Figure 5: Steps to create a CBGS using unclassified LiDAR points

A three-meter grid surface is created using the raw LiDAR points, assuming that at least one point belongs to the ground surface. Every grid is assigned the lowest elevation within the grid, assuming that it belongs to the ground surface. The grid size is determined based on the average point density and the size of objects in the area. To increase the point density and close resemblance to the actual ground surface, all the LiDAR points within 0.5 m of this raster surface are classified as bare ground points.

A close, examination of the grid surface reveals that several grids over the water surface are without any points due to the sparseness of LiDAR points; hence they are labeled as "no elevation grid" (NE-grid). Similarly, several other grids contained very few points; 1 or 2 compared to the average point density of 162 points per 9 m^2. Close inspection of these grids revealed that these points either belonged to the water surface, and are the result of complete absorption of the SP LiDAR pulse. Therefore, grids with less than 3 points are also labeled NE-grid and the points over these grids are classified as non-ground.

The NE-grid cells are assigned a low elevation so that they resemble the under water surface. We refer to this process as "river surface burning" [3]. This process removes the undesirable triangulation effects. This method is an extension of the process known as river burning[5], which is used for linear features. A TIN surface is created using the bare ground points and the NE-grid points. This surface is called the continuous bare ground surface (CBGS) in this paper.

4.2 Water surface extraction and bank shoreline extraction

The VWS determination of SP LiDAR is different when compared to LM LiDAR because the SP LiDAR works at a wavelength of 0.532 microns. Due to the use of this wavelength, elevation points are available on and underneath the water surface because the pulses penetrate the water surface. The following section explains the methodology to create a VWS using a SP-LiDAR point cloud.

4.2.1 VWS creation

To determine the water surface elevation, it is assumed that at least 1 water surface point exists in a 3 m $\times$ 3 m area. A raster grid of 3 m $\times$ 3 m is created using the maximum point elevation within each grid. The NHD river centerline is converted to 3D using this surface. Figure 6 shows the elevation variation along the centerline of the Connecticut river. Points along and below the water surface and over the two bridges can be seen in this figure. Structures over the water surface are removed manually to produce

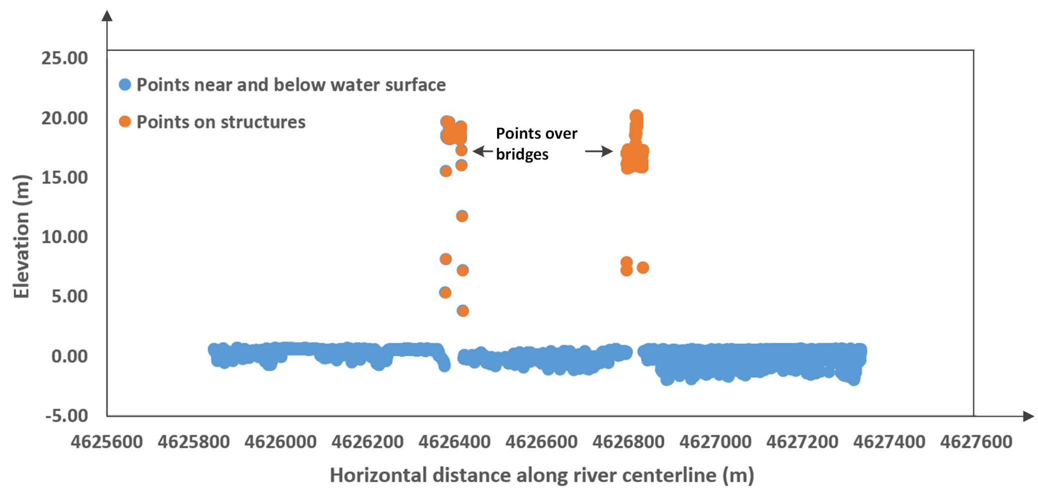

Figure 6: Elevation profile of the river centerline from the 3 m raster grid of SP LiDAR

a elevation profile, as shown in Figure 7. It is necessary to fulfill hydro-flattening requirements by maintaining hydrologic connectivity. Hence, a check, similar to the LM LiDAR data, is implemented at each point along the centerline from D/S to U/S to eliminate drop points and low outliers. According to this check, if the elevation of a point is less than its D/S point, this point is assigned the D/S point's elevation. Figure 7 shows the revised water surface elevations used at the respective cross-sections to create the B-VWS.

The B-VWS is very close to the CBGS surface. Hence, it is raised based by 0.5 m based on a study performed in [3]. Figure 8 shows an example of the longitudinal profile of a river with different water surfaces features. It also indicates that due to the slope of the water surface between the two cross-sections, the B-VWS is below the actual water surface by a height of x. The LiDAR point cloud may or may not record some of the real water surface features such as small protruding objects, surface ripples, waves, broken tree branches, etc. These features are labeled as ΔV. LiDAR data over other study was used in this research to determine the rise necessary to include water surface variations.

The B-VWS is revised by adding 0.5 m to create a Intersection-VWS (I-VWS). This surface is intersected with the CBGS surface to extract the bank

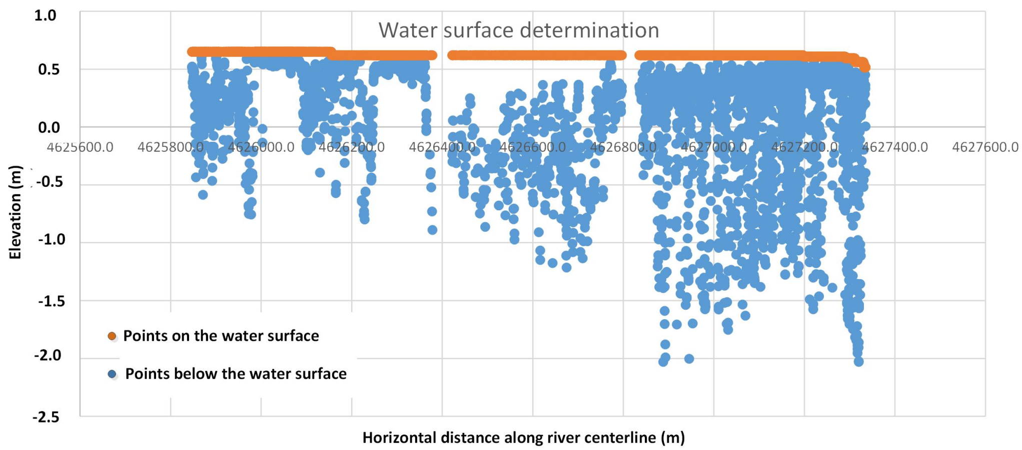

Figure 7: Elevations profile of the river centerline from the 3 m raster grid of SP LiDAR

shoreline at the time of data acquisition. Figure 9(b) shows the raw bank shoreline obtained by the surface intersection. A smoothing and filtering process is implemented to fill voids smaller than 200 m^2 and to smooth the boundary using PAEK method with a threshold value of 30.48 m (100 ft) to obtain a smoothed bank shoreline as shown in Figure 9(c). This line is manually edited to connect over the bridges.

5 Results

The edited bank shoreline, determined in the previous step is converted to 3D by assigning elevations from the B-VWS. The SP-LiDAR points between the shorelines are classified as water points. In addition, points within 0.5 m from the shorelines were identified as Ignored ground points (class value of 10) [4]. Both the water points and the Ignored ground points are excluded and the remaining bare ground points were triangulated using the 3D bank shoreline to develop a SP-LiDAR based hydro-flatten DEM.

Figure 10 shows the results obtained for the Connecticut River. Visual comparison shows that the bank shoreline aligns with the bank shoreline from the orthoimage. In addition the water surface profile also shows a consistent drop in elevation along the centerline.

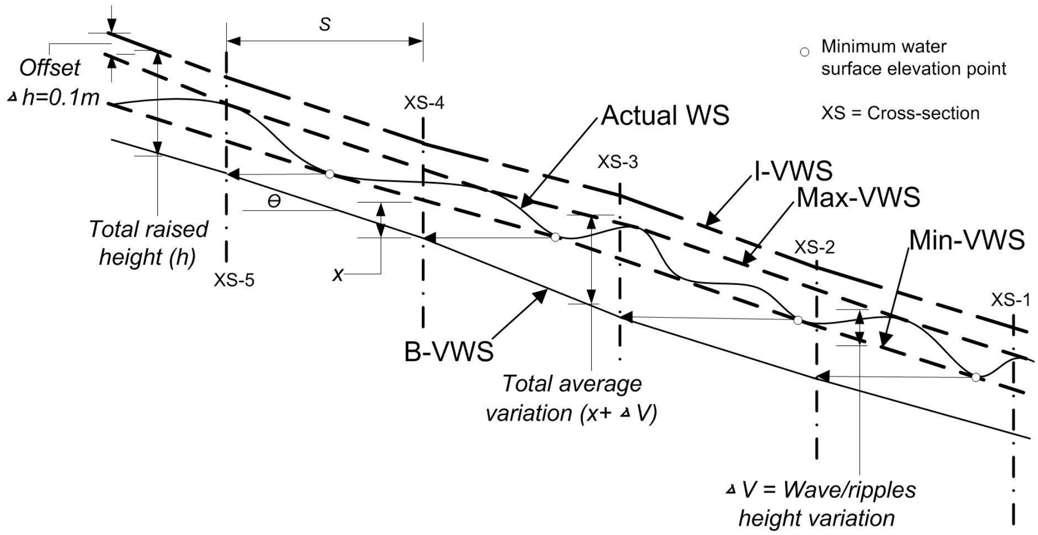

Figure 8: Water surface profile of river showing water surface variation, B-VWS, and I-VWS [3]

6 Conclusion

In this paper, we have presented a semi-automatic method to create a SP-LiDAR based hydro-flattened DEM using the elevation information of the SP-LiDAR. We have presented the implementation using a raw point cloud provided by Sigma Space corporation. First, a bare ground surface was created. An approximate river centerline was used as an approximate location. Elevations along this centerline were extracted from the all point surface and was processed to extract a water surface profile at the time of data acquisition. Cross-sections were placed at right angles to the river centerline and elevations from the revised river centerline were used to create a water surface. Using the water surface analysis performed in an earlier study, a 0.5 m height was added to the water surface. This surface was intersected with the bare ground points to extract the shoreline. This method is useful for filling gaps in water areas. This implementation supports the addition of 0.5 m to the B-VWS without performing water surface feature analysis. Furthermore, the search radius and the cross-section spacing of $1.5 \times W$ was able to extract bank shoreline for both rivers despite the fact that they differ significantly in slope and width. The B-VWS, which is used to obtain height information,

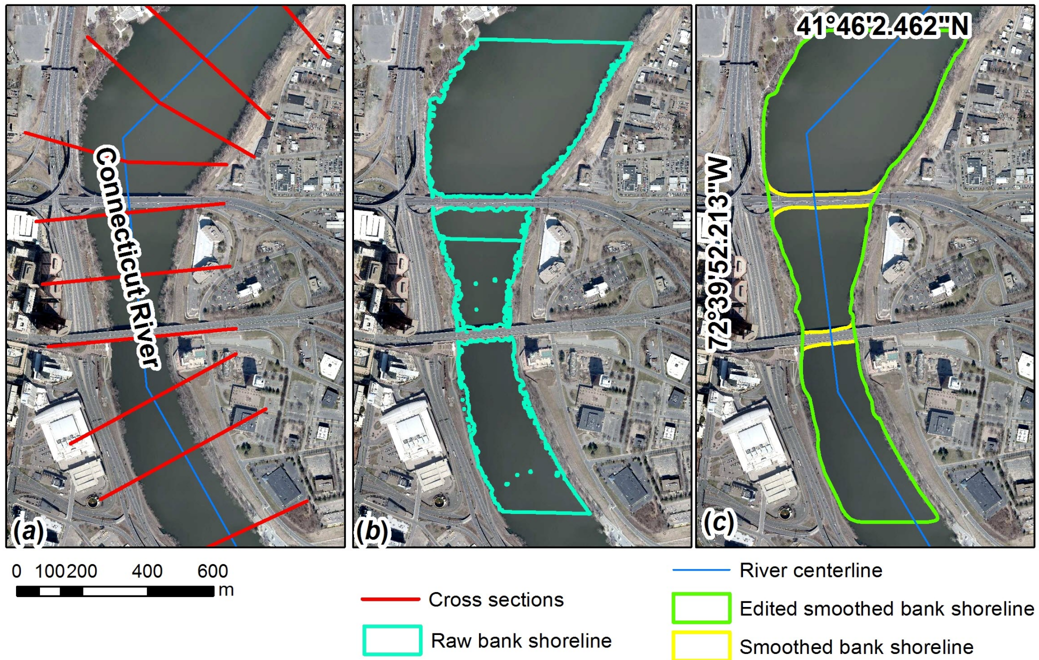

Figure 9: Bank shoreline along the river. (a) shows the river centerline and the cross-sections, (b) shows the raw bank shoreline extracted by the surface intersection, and (c) shows the smoothed and edited bank shoreline.

showed a gradual drop in elevation conforming to the USGS requirement of Hydro-flattening.

Acknowledgment

This research was supported by the faculty development grant at the Ferris State University. We would like to thank the Sigma Space corporation for providing the SP LiDAR data.

References

[1] Qassim A Abdullah. A star is born: The state of new lidar technologies. *Photogrammetric engineering & remote SenSing*, 82(5):307–312, 2016.

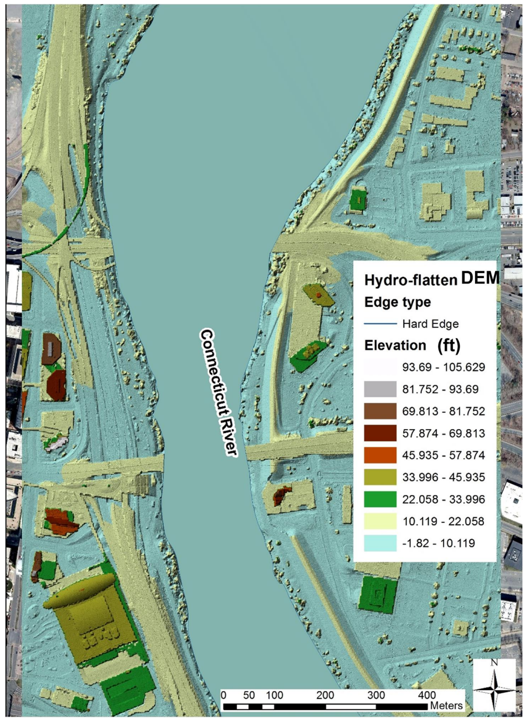

Figure 10: Hydro-flattened DEM surface created using Single photon LiDAR

[2] A. S. Antonarakis, K. S. Richards, and J. Brasington. Object-based land cover classification using airborne lidar. *Remote Sensing of Environment*, 112(6):2988–2998, 2008.

[3] S S Deshpande and A Yilmaz. A semi-automated method to create a lidar-based hydro-flattened dem. *International Journal of remote sensing*, 38(5):1365–1387, 2017.

[4] H. K. Heidemann. Lidar base specification. 2012.

[5] GF Koltun, S. P. Kula, and B. M. Puskas. A streamflow statistics (streamstats) web application for ohio. Technical report, US Department of the Interior, US Geological Survey, 2006.

[6] George Sithole and George Vosselman. Experimental comparison of filter algorithms for bare-earth extraction from airborne laser scanning point

clouds. *ISPRS journal of photogrammetry and remote sensing*, 59(1):85–101, 2004.

[7] Sigma Space. HRQLS High resolution quantum LiDAR System, Sample Data: December 2015. Technical report, Sigma Space, USA., 2015.

[8] James Wilder Young. We may be a lot closer than we originally thought! *LIDAR magazine*, 5(5):1–5, 2016.